



**HAL**  
open science

# Using a high finesse optical resonator to provide a long light path for differential optical absorption spectroscopy: CE-DOAS

J. Meinen, J. Thieser, U. Platt, T. Leisner

► **To cite this version:**

J. Meinen, J. Thieser, U. Platt, T. Leisner. Using a high finesse optical resonator to provide a long light path for differential optical absorption spectroscopy: CE-DOAS. Atmospheric Chemistry and Physics Discussions, 2008, 8 (3), pp.10665-10695. hal-00304229

**HAL Id: hal-00304229**

**<https://hal.science/hal-00304229>**

Submitted on 18 Jun 2008

**HAL** is a multi-disciplinary open access archive for the deposit and dissemination of scientific research documents, whether they are published or not. The documents may come from teaching and research institutions in France or abroad, or from public or private research centers.

L'archive ouverte pluridisciplinaire **HAL**, est destinée au dépôt et à la diffusion de documents scientifiques de niveau recherche, publiés ou non, émanant des établissements d'enseignement et de recherche français ou étrangers, des laboratoires publics ou privés.

High finesse optical  
resonators for DOAS  
measurements

J. Meinen et al.

# Using a high finesse optical resonator to provide a long light path for differential optical absorption spectroscopy: CE-DOAS

J. Meinen<sup>1,2</sup>, J. Thieser<sup>2</sup>, U. Platt<sup>2</sup>, and T. Leisner<sup>1,2</sup>

<sup>1</sup>Institute for Meteorology and Climate Research, Aerosols and Heterogeneous Chemistry in  
the Atmosphere (IMK-AAF), Forschungszentrum Karlsruhe GmbH, Germany

<sup>2</sup>Institut for Environmental Physics (IUP), Atmosphere and Remote Sensing,  
Ruprecht-Karls-Universität Heidelberg, Germany

Received: 17 April 2008 – Accepted: 9 May 2008 – Published: 4 June 2008

Correspondence to: J. Meinen (jan.meinen@imk.fzk.de)

Published by Copernicus Publications on behalf of the European Geosciences Union.

Title Page

Abstract

Introduction

Conclusions

References

Tables

Figures

◀

▶

◀

▶

Back

Close

Full Screen / Esc

Printer-friendly Version

Interactive Discussion



## Abstract

Cavity enhanced methods in absorption spectroscopy have seen a considerable increase in popularity during the past decade. Especially Cavity Enhanced Absorption Spectroscopy (CEAS) established itself in atmospheric trace gas detection by providing tens of kilometers of effective light path length using a cavity as short as 1 m. In this paper we report on the construction and testing of a compact and power efficient light emitting diode based broadband Cavity Enhanced Differential Optical Absorption Spectrometer (CE-DOAS) for in situ field observation of atmospheric NO<sub>3</sub>. This device combines the small size of the cavity with the enormous advantages of the DOAS approach in terms of sensitivity and specificity. In particular, no selective removal of the analyte (here NO<sub>3</sub>) is necessary, thus the CE-DOAS technique can – in principle – measure any gas detectable by DOAS. We will discuss the advantages of using a light emitting diode (LED) as light source particularly the precautions which have to be satisfied for the use of LEDs. The instrument was tested in the lab by detecting NO<sub>3</sub> in a mixture of NO<sub>2</sub> and O<sub>3</sub> in air. It was then compared to other trace gas detection techniques in an intercomparison campaign in the atmosphere simulation chamber SAPHIR at NO<sub>3</sub> concentrations as low as 6.3 ppt.

## 1 Introduction

Optical absorption spectroscopy is commonly used for trace gas analysis in ambient air since it is a direct, in situ, non-invasive approach to quantify concentrations of gaseous trace species and aerosol. Every absorption spectroscopy methodology makes use of the Lambert-Beer's law:

$$I(\lambda) = I_{in}(\lambda) \times \exp[-\sigma(\lambda) \times c \times L] = I_{in}(\lambda) \times \exp[-\alpha(\lambda) \times L] \quad (1)$$

Where  $I_{in}(\lambda)$  and  $I(\lambda)$  are the light intensity of the source and the intensity after the light has propagated the distance  $L$  through an absorbing medium, respectively. The absorb-

## High finesse optical resonators for DOAS measurements

J. Meinen et al.

Title Page

Abstract

Introduction

Conclusions

References

Tables

Figures

⏪

⏩

◀

▶

Back

Close

Full Screen / Esc

Printer-friendly Version

Interactive Discussion



**High finesse optical resonators for DOAS measurements**

J. Meinen et al.

ing medium has the absorptivity  $\alpha(\lambda)$ , which is represented by a concentration  $c$  of an absorber with the absorption cross section  $\sigma(\lambda)$ . By the application of cavity enhanced light paths in absorption spectroscopy of atmospheric trace gases the detection limits were successfully lowered to sufficient values because the signal increases with the length of the light path  $L$ .  $L_0$  is the length of a light path inside an empty resonator consisting of two highly reflective mirrors of reflectivity  $R$  separated by the distance  $d_0$ .  $L_0$  has to be interpreted as the average light path over all photons or partial rays propagating inside the resonator before they leave it by passing one of the mirrors. This value can be estimated by:

$$L_0 \approx \frac{d_0}{1 - R} \quad (2)$$

The mirror reflectivity is commonly  $R \approx 0.999 \dots 0.999985$  providing a light path  $L_0 \approx 1 \dots 60$  km suitable for a detection limit of  $\alpha \leq 1 \times 10^{-9} \text{ cm}^{-1}$  or below.

There are two basic approaches for cavity enhanced spectrometry relying on a pumped optical resonator: Eq. (1) Cavity Ring-Down Spectroscopy (CRDS) measures the decay of light intensity leaking from the resonator after switching off the pump and therefore is a time dependent measurement. Equation (2) Cavity Enhanced Absorption Spectroscopy (CEAS) measures the transmittance of the resonator by recording the leak-out intensity. Both techniques are reviewed e.g. by Ball et al. (2003) and Brown (2003).

In Cavity Ring-Down Spectroscopy, the change in the  $1/e$  decay time of the resonator is measured to determine the absorbance  $\alpha$  of a sample. This is an elegant calibration free approach, but the decay time of the empty resonator has to be known. So there is the problem of removing the absorber, which can cause difficulties in field use. One approach is to remove the analyte by titration and to monitor the corresponding change in transmission. The second approach is to use two detection channels: One at the centre of an absorption line and the other at a region of the spectrum where the absorption line is weak. Both approaches are markedly vulnerable to the background extinction and thus only feasible with a very limited number of species of atmospheric

[Title Page](#)[Abstract](#)[Introduction](#)[Conclusions](#)[References](#)[Tables](#)[Figures](#)[◀](#)[▶](#)[◀](#)[▶](#)[Back](#)[Close](#)[Full Screen / Esc](#)[Printer-friendly Version](#)[Interactive Discussion](#)

interest.

A great improvement was the introduction of Broadband CRDS (BB-CRDS) in 2001 (see review of Ball et al., 2003). This technique provides wavelength resolved absorption spectra, which can be analyzed by fitting routines known from the established Differential Optical Absorption Spectroscopy (DOAS) as introduced by Platt and Perner (1980).

A parallel development was the continuous wave operation of the resonator, first introduced as Cavity Enhanced Absorption Spectroscopy (CEAS) by Engeln et al. (1998). This approach takes advantage of the extension of the absorption light path within the resonator similar to white (White, 1942) or herriot (Herriot et al., 1965) cells. CEAS uses the integrated leak-out intensity of a beam propagating between two highly reflective mirrors. The absorption coefficient  $\alpha$  within the cavity can be related to the leak-out intensity once the amount of light coupled into the resonator and the mirror reflectivity is known. With some basic approximations a simple formula can be derived (Fiedler et al., 2003):

$$\alpha = \frac{1}{d_0} \left( \frac{I_0}{I} - 1 \right) (1 - R) \quad (3)$$

Here  $I_0$  and  $I$  are the intensities transmitted through the empty resonator (i.e. filled with pure, synthetic air) and the resonator with an absorbing species inside, respectively. Note that the determination does not rely on the knowledge of the intensity  $I_{in}$  coupled into the resonator. We will show in a forthcoming publication<sup>1</sup> that this approximated formula and even its more general form derived in Fiedler et al. (2003) is only valid in the case of small extinction. This phenomenon was already observed by other authors (Langridge et al., 2006) who found an increasing underestimation of their target gas

<sup>1</sup> Platt, U., Meinen, J., Pöhler, D., and Leisner T.: Broadband Cavity Enhanced Absorption Spectroscopy (CEAS), how to determine the correct light-path length for DOAS measurements. To be referred as “theory paper”.

**High finesse optical resonators for DOAS measurements**

J. Meinen et al.

Title Page

Abstract

Introduction

Conclusions

References

Tables

Figures

◀

▶

◀

▶

Back

Close

Full Screen / Esc

Printer-friendly Version

Interactive Discussion



concentration with higher concentration of the analyte without a substantiated explanation of this deviation.

With the development of the incoherent broad-band CEAS (IBB-CEAS) by Fiedler et al. (2003), trace gas analysis with CEAS became feasible. As in BB-CRDS, a wavelength resolved absorption spectrum is obtained from Eq. (3). Column densities of the absorbing trace species are then determined by differential fitting which is the well known DOAS approach (Platt et al., 1980). For the retrieval of concentrations from column densities the quality of the resonator (represented by  $R$  in Eq. 3 or the  $L_0$  in Eq. 2) has to be determined. Broadband devices either rely on separate measurement of the empty cavity or simultaneously determine the absorptions of absorbers with known concentrations (e.g.  $H_2O$ ,  $O_2$ ,  $O_4$ , Platt et al., 1980) as it was introduced in 2004 for DOAS approaches (Hönninger et al., 2004). In this contribution we use a more direct way to define the light path  $L_0$  by employing CRD parallel to recording broadband transmission spectra. The theoretical background of this procedure will be the scope of the above mentioned theory paper.

In comparison to the single wavelength approach particular advantages of the DOAS approach (Platt et al., 1980) include very high sensitivity and selectivity of the measurement<sup>2</sup>. Both properties are owed to the simultaneous recording of the intensity transmitted by the cavity at many different wavelengths, allowing the detection of very weak absorption bands (optical densities of  $10^{-3}$  or below). By separating narrow-band “differential” absorption structures due to trace gas molecules from intensity changes which are smoothly varying with wavelength, like changes in mirror reflectivity or Mie scattering from aerosol, the latter effects can be eliminated. The recorded spectra usually encompass several absorption bands of the trace species of interest, thus detection becomes very specific and reliable. In fact, even overlapping absorption structures of several species can usually be de-convoluted, which is impossible with the single wavelength approach. Numerous examples of applying this procedure in field

<sup>2</sup> This will be discussed in great detail in “The DOAS book”: Platt, U. and Stutz, J.: Differential Optical Absorption spectroscopy, Principles and Applications. Springer, Heidelberg, in press.

## High finesse optical resonators for DOAS measurements

J. Meinen et al.

Title Page

Abstract

Introduction

Conclusions

References

Tables

Figures

◀

▶

◀

▶

Back

Close

Full Screen / Esc

Printer-friendly Version

Interactive Discussion



measurements are reported in the literature and will be summarized in the above mentioned DOAS book. As a consequence, no selective removal of the trace gas of interest (by e.g. titration) is required, which allows universal application of our technique in field and laboratory measurements of all trace gases measurable by DOAS, including NO<sub>2</sub>, SO<sub>2</sub>, halogen oxides and aromatics (e.g. Platt et al., 1980 and “The DOAS book”). Moreover, due to the immunity to aerosol scattering, measurements in the open air are possible.

We present here an easy to use cavity enhanced spectrometer, especially designed for direct use in combination with classical DOAS instruments. This results in a robust and cost-efficient device for field use comparable to Mini-MAX-DOAS devices (Hönninger, 2004). The device was compared to other cavity enhanced systems and alternative approaches for trace gas detection at an intercomparison campaign<sup>3</sup> and showed good performance compared to more complicated and costly instruments. For uniformity in nomenclature we call this approach Cavity Enhanced DOAS (CE-DOAS).

## 2 Experimental

The instrument (see Fig. 1) consists of a LED as a light source, a resonator formed by two highly reflective mirrors ( $M_1$ ,  $M_2$ ), a fiber coupler to collect light leaking through mirror  $M_2$  and either a fiber coupled photomultiplier (PMT) or a fiber coupled spectrograph with a charge coupled device (CCD) camera for time resolved or wavelength dispersed measurements respectively. As detailed in the text below, the light source is driven by a function generator in combination with a HF amplifier or by a constant current source, depending whether time resolved ring-down measurements or wavelength dispersed intensity measurements are desired.

<sup>3</sup>Dorn, H. P., Brauers, T., Meinen, J., et al.: Intercomparison of NO<sub>3</sub> radical detection techniques in the atmosphere simulation chamber SAPHIR., to be submitted to Atmos. Chem. Phys. Discuss., 2008.

### High finesse optical resonators for DOAS measurements

J. Meinen et al.

Title Page

Abstract

Introduction

Conclusions

References

Tables

Figures

◀

▶

◀

▶

Back

Close

Full Screen / Esc

Printer-friendly Version

Interactive Discussion



---

**High finesse optical resonators for DOAS measurements**J. Meinen et al.

---

[Title Page](#)[Abstract](#)[Introduction](#)[Conclusions](#)[References](#)[Tables](#)[Figures](#)[⏪](#)[⏩](#)[◀](#)[▶](#)[Back](#)[Close](#)[Full Screen / Esc](#)[Printer-friendly Version](#)[Interactive Discussion](#)

The use of a LED offers considerable advantages with respect to size, complexity and robustness. Previous instruments either suffer from a bulky light source like a pulsed laser source (e.g. Ball et al., 2001), a dye laser system (e.g. Ball et al., 2003 and Brown, 2003) or a Xe-Arc lamp (e.g. Hamers et al., 2002 and Fiedler et al., 2003). As some other authors did before (e.g. Ball et al., 2004), we utilized the rapid improvement of the light emitting diode (LED) technology. LEDs are cheap, light weight, and sufficiently stable in emission to be used for absorption spectroscopy. Conveniently, their emission bandwidth is similar to the wavelength range of typical high reflective mirrors. Furthermore the need for mode matching, off-axis alignment or dithering the frequency space of the optical resonator is avoided by the incoherent emission of the LED (e.g. Simpson 2003, Paul et al., 2001 and O'Keefe et al., 1999, respectively). The performance of LED driven instruments is still limited by their surface luminance, even though it has increased by orders of magnitudes in recent years. We found by ray tracing simulation, that for stable trapping of a light beam in the resonator its input beam divergence has to be smaller than  $0.5 \text{ mrad}$ <sup>4</sup>. One can easily estimate under these conditions that the LED radiating area actually imaged into the resonator is of the order of  $200 \times 200 \mu\text{m}$ . This is probably one reason why many authors report a poor coupling efficiency (Ball et al., 2004). It is therefore not essential to use a high total power LED, which gains its power not from high surface luminance but rather from a large emitting area. For the wavelength region required, the LED TO3A4-H660-180 (Roithner Lasertechnik GmbH, Austria) was found to perform well. At  $25^\circ\text{C}$  this LED has sufficient surface luminance of  $65 \text{ mW}/\text{mm}^2$ , its emission spectrum exhibits a nearly Lorentzian shape peaking at  $665 \text{ nm}$  with a width of  $23 \text{ nm}$  (FWHM) and shows little etalon structure, which is essential for differential fitting.

In this setup, the most effective coupling of the LED light in and out of the resonator was achieved by placing the resonator in between a two lens optics ( $L_1=L_2$ :  $f=40 \text{ mm}$ ,

---

<sup>4</sup> Meinen, J.: Design and assembling of a broadband cavity ringdown and cavity enhanced absorption spectrometer using light emitting diodes., Thesis, Technical University of Ilmenau, Germany, 108 pp., 2007.

see Fig. 1). No modification of the LED and no fiber optics are required with this setup. The emission spectrum of the LED includes not only the 662 nm band, where the measurement is performed, but also the 624 nm absorption band of  $\text{NO}_3$ , which is vulnerable to photolysis. Thus a 3 mm RG610 (Schott, Germany) filter is inserted between the resonator and the light source. The optical net power at the outer surface of the inlet mirror  $M_1$  was determined to be about  $150 \mu\text{W}$ .

While all LEDs show a shift in peak wavelength with changing temperature, some LED spectra additionally contain super-imposed periodic structures caused by a Fabry-Perot etalon effect. The wavelengths at which constructive interference occurs are dependent on the thickness and refractive index of the layers of different materials inside the LED. Because these properties are temperature dependent themselves, the etalon structure changes its spectral position with changing temperature (Kern et al., 2006). A highly stable temperature and emitter current control device was used to minimize shifts in the etalon structure of the LEDs thereby providing a light source well appropriated for differential fitting analysis. For ring-down measurements, a function generator (Model 7060 Generator, Exact Electronics Inc., ORE, USA) was used to trigger a UHF transistor (2N3733) which was interconnected between the current source and the LED. With this setup the edge steepness of the LED light pulse was  $<0.8 \mu\text{s}$  at a repetition rate of 770 Hz.

The resonator consisted of two high reflective mirrors (Los Gatos Research, Inc., USA) with a nominal reflectivity of 99.9985% at 655 nm, 25.4 mm diameter and 1 m radius of curvature. The length  $d_0$  of the cavity was 620 mm. A fraction of this distance between the mirrors was required for a mirror purge system realized by a counter flow of dry, filtered air (see Fig. 1). It was dimensioned to leave an effective absorption path length  $d_{\text{eff}}=(500\pm 12)$  mm. The characteristic of the flow inside the cavity was optimized by means of computational fluid dynamic (CFD) calculations (ANSYS-CFX, ANSYS, Inc., USA). Typical optical path lengths achieved in the given resonator were between 15 and 20 km. This is a somewhat lower value than expected from the nominal mirror reflectivity, which yields a light path in the region of 40 km. Rayleigh scattering

## High finesse optical resonators for DOAS measurements

J. Meinen et al.

Title Page

Abstract

Introduction

Conclusions

References

Tables

Figures

◀

▶

◀

▶

Back

Close

Full Screen / Esc

Printer-friendly Version

Interactive Discussion



of N<sub>2</sub> reduces the maximum possible light path to a value of about 33 km in this configuration (Sneep et al., 2005). There is still an apparent additional absorbance of about  $\alpha=2\times 10^{-7} \text{ cm}^{-1}$  which indicates degraded mirror surfaces. As the optimal light path for our application is in the region of 12 km anyhow, (see Sect. 3.2), we did not try to optimize the mirror reflectivity.

The alignment of the resonator was checked with a CCD camera (SensiCam, PCO imaging) equipped with a 25 mm video lens (Cosmicar/Pentax TV-Lens, 25 mm, 1:1.4). When the image at the output mirror surface was a well defined circle with maximized diameter, transmission was best. This alignment of the lenses corresponds to a focal plane centered between the two mirrors, as described by other authors before (Fiedler et al., 2007). The exit beam diameter in the focal plane of  $L_2$  was measured with the CCD camera to be about 1.6 mm. An optical fiber ( $d=400 \mu\text{m}$ , NA=0.2) was placed in the focal spot to guide the light into the detection unit.

For time resolved measurements the cavity output was guided into the PMT (H5783-01, Hamamatsu Photonics Germany GmbH, Hersching) which was operated in continuous current mode. The current was amplified by a fast current to voltage amplifier (DLPCA 200, FEMTO Messtechnik GmbH, Berlin) and digitized by a fast digital oscilloscope (DAQSCOPE PCI-5102, National Instruments Germany GmbH, München). Data recording and processing was managed by LabView software (LabView 8.2, National Instruments Corporation, USA).

Wavelength dispersed measurements were performed with a Czerny Tuner spectrograph (USB 2000, Ocean Optics, Inc., USA) equipped with a CCD array (Sony ILX 511 linear silicon CCD array, 2048 pixels) with a spectral resolution of 1.06 nm (ca. 6,5 pixel at FWHM) to acquire the spectra. The acquisition rate was limited by exposure and readout time to approximately  $0.2 \text{ min}^{-1}$ . Optical bench and detector of the spectrograph were cooled down to approximately  $0^\circ\text{C}$  in a Mini-DOAS housing (see Hönninger et al., 2004). While taking the spectra, the exposure time was varied automatically to reach constant modulation amplitude for each spectrum. Typically, the exposure time was about 60 s. The spectra are handled and evaluated by using the DOASIS software

## High finesse optical resonators for DOAS measurements

J. Meinen et al.

Title Page

Abstract

Introduction

Conclusions

References

Tables

Figures

◀

▶

◀

▶

Back

Close

Full Screen / Esc

Printer-friendly Version

Interactive Discussion



(Kraus, 2006). For future experiments we plan to enhance the overall performance and temporal resolution using a more sensitive spectrometer with faster readout electronics, more efficient fiber coupling at the exit of the resonator a more powerful light source (see Sect. 5).

## 5 2.1 Modification for operation in the SAPHIR chamber

Since  $\text{NO}_3$  is a very unstable radical, inlet losses on sample line and cavity housing can potentially cause substantial errors in absolute concentration. Therefore the resonator was placed directly inside the SAPHIR chamber without any tube or housing between the mirrors (open path configuration). This possibility is one of the inherent advantages of the CE-DOAS method. The mirrors were purged by 5 l/min synthetic air to avoid degradation of the reflectivity during the measurement. A fan placed besides the cavity ensures sufficient circulation of fresh sample air between the mirrors and avoids dilution of the analyzed air due to the purge flow, a prerequisite which presumably would not be necessary in the field due to the always present motion of the air. The LED-light source was directly attached to the resonator inside the chamber but the detection system was kept outside the chamber and was connected to the resonator via a 5 m long quartz fiber ( $D=400 \mu\text{m}$ ,  $\text{NA}=0.22$ ).

## 3 Data evaluation

Data evaluation was performed in two steps:

1. Determination of the distance the light travels inside the empty resonator (optical path length  $L_0$ ). This can be achieved by measuring the attenuation constant of the ring-down signal when the cavity is purged. This procedure is described in detail in section 3.1.
2. Determination of the column densities  $D'$  of the different absorbers in the resonator, which is achieved by differential fitting. Absorber concentrations  $c$  can be

### High finesse optical resonators for DOAS measurements

J. Meinen et al.

Title Page

Abstract

Introduction

Conclusions

References

Tables

Figures

◀

▶

◀

▶

Back

Close

Full Screen / Esc

Printer-friendly Version

Interactive Discussion



calculated from  $L_0$  and  $D'$  including pressure and temperature by the ideal gas law. This procedure is described in Sect. 3.2.

### 3.1 Determination of the optical path length $L_0$

For determination of the optical path length the cavity was flushed with dry filtered nitrogen in laboratory use and with synthetic air during an intercomparison campaign detailed below, assuming finite reflectivity and Rayleigh scattering by nitrogen were the only processes acting to attenuate light within the cavity. 1000 ring-down events were processed by a floating average algorithm to reduce noise and an exponential function was fitted to the data (see Fig. 2, dashed line). A typical ring-down event with total exposure time of 1.3 s is shown.

Figure 2 shows the nonlinearity of the logarithm of the ring-down signal due to the summation of varying light paths at different wavelengths covered by the LED emission spectrum. Since the reflectivity of the mirrors peaks at 655 nm and decreases substantially at the edges of the emission spectrum of the light source, the distance light travels between the mirrors depends considerably on wavelength. This effect becomes even more pronounced, when an absorber with an absorption line narrower than the LED emission spectrum is inside the resonator. In these cases, a simple exponential fit is not suitable for the determination of the light path any more. The time dependent signal  $S(t)$  has to be modeled by an integral over the wavelength:

$$S(t) = I_0 \int I(\lambda) \times \exp \left[ -\frac{c}{L_0(\lambda)} \times t \right] d\lambda + b \quad (4)$$

Where  $I_0$  is the transmitted intensity at  $S(t=0)$ ,  $I(\lambda)$  is the normalized emission spectrum of the LED,  $L_0(\lambda)$  is the wavelength dependent light path in the cavity given by the mirror reflectivity  $R(\lambda)$  according to Eq. (2) and  $b$  is a baseline. A detailed discussion including the effect of absorber species inside the cavity is given in the above mentioned thesis of Meinen. In the special case of our mirrors, which have their peak reflectivity

## High finesse optical resonators for DOAS measurements

J. Meinen et al.

Title Page

Abstract

Introduction

Conclusions

References

Tables

Figures

◀

▶

◀

▶

Back

Close

Full Screen / Esc

Printer-friendly Version

Interactive Discussion



centered at the 655 nm NO<sub>3</sub> absorption band, this effect is not very pronounced. Simulations with Eq. (4) show that fitting a mono-exponential function between 5 μs and 75 μs to the signal of the empty cavity allows to determine a wavelength independent L<sub>0</sub>. In doing so the error remains below 3%.

### 5 3.2 Differential Broadband Absorption

DOAS makes use of Lambert-Beer's law (Eq. 1) to determine the average trace gas concentration *c*. Radiation with the initial intensity *I<sub>in</sub>(λ)* is emitted by the source, *I(λ)* is the radiation intensity after passing through a layer of thickness *L*, where the absorber is present. The quantity *σ(λ)* denotes the absorption cross section as function of wavelength *λ*.

As the radiation propagates through air, its intensity is reduced through the absorption of a specific trace gas. However, it also undergoes extinction due to absorption processes by other trace gases, and scattering by air molecules and aerosol particles. The finite eidelbergity of the instrument will also decrease the light intensity. Therefore the simple Lambert-Beer's law (Eq. 1) has to be expanded to consider the various factors that influence the radiation intensity. The absorption of several trace gases with concentration *c<sub>j</sub>* and absorption cross sections *σ<sub>j</sub>(λ)*, Rayleigh and Mie extinction, *ε<sub>R</sub>(λ)* and *ε<sub>M</sub>(λ)* and instrumental effects summarized in *T(λ)*:

$$I(\lambda) = I_{in}(\lambda) \times \exp \left[ -L \times \left( \sum_j (\sigma_j(\lambda) \times c_j) + \varepsilon_R(\lambda) + \varepsilon_M(\lambda) \right) \right] \times T(\lambda) \quad (5)$$

In order to determine the concentration of a particular trace gas it would be necessary to quantify all other factors influencing the intensity. While previous CEAS and CRDS experiments selectively removed the absorber from the light path this does not appear practical in many cases.

The application of Differential Optical Absorption Spectroscopy overcomes this challenge by using the fact that aerosol extinction processes, instrumental effects, and

## High finesse optical resonators for DOAS measurements

J. Meinen et al.

Title Page

Abstract

Introduction

Conclusions

References

Tables

Figures

◀

▶

◀

▶

Back

Close

Full Screen / Esc

Printer-friendly Version

Interactive Discussion



many trace gas absorptions show very broad or even smooth spectral characteristics. Certain trace gases, however, exhibit narrow band absorptions structures. The foundation of DOAS is thus to separate broad and narrow band spectral structures in an absorption spectrum in order to isolate these narrow trace gas absorptions (Platt et al., 1980). The broad spectrum is then used as a new intensity spectrum  $I_{in}'(\lambda)$ , and Lambert-Beer's law can again be applied to the narrow band trace gas absorptions. Accordingly, we split the absorption cross section:

$$\sigma_j(\lambda) = \sigma_{j0}(\lambda) + \sigma'_j(\lambda) \quad (6)$$

$\sigma_{j0}$  in Eq. (6) varies "slowly" with the wavelength  $\lambda$ , for instance describing a general 'slope', such as that caused by Rayleigh and Mie scattering, while  $\sigma'_j$  shows rapid variations with  $\lambda$ , for instance due to an absorption band. The division between 'rapid' and 'slow' variations is ambiguous and depends on the observed wavelength interval and the width of the absorption bands to be detected. Inserting Eq. (6) into Eq. (5) we obtain:

$$I(\lambda) = I_{in}'(\lambda) \times \exp \left[ -L \times \left( \sum_j (\sigma'_j(\lambda) \times c_j) \right) \right] \times \exp \left[ -L \times \left( \sum_j (\sigma_{j0}(\lambda) \times c_j) + \varepsilon_R(\lambda) + \varepsilon_M(\lambda) \right) \right] \times T(\lambda) \quad (7)$$

The first exponential function in Eq. (7) describes the effect of the structured 'differential' absorption of a trace species, while the second exponential (including  $T(\lambda)$ ) constitutes the slowly varying absorptions, as well as the influence of Rayleigh and Mie scattering (however the influence of broad-band absorptions on  $L$  does need to be taken into account as we will show in the above mentioned theory paper. With the quantity  $I_{in}'$  as

**High finesse optical resonators for DOAS measurements**

J. Meinen et al.

Title Page

Abstract

Introduction

Conclusions

References

Tables

Figures

◀

▶

◀

▶

Back

Close

Full Screen / Esc

Printer-friendly Version

Interactive Discussion



the intensity in the absence of differential absorption

$$I'_{in}(\lambda) = I_{in}(\lambda) \times \exp \left[ -L \times \left( \sum_j (\sigma_{j0}(\lambda) \times c_j) + \varepsilon_R(\lambda) + \varepsilon_M(\lambda) \right) \right] \times T(\lambda) \quad (8)$$

we obtain:

$$\frac{1}{L} \times \ln \left[ \frac{I'_{in}(\lambda)}{I(\lambda)} \right] = \sum_j \sigma'_j(\lambda) \times c_j \quad (9)$$

5 The intensity  $I'_{in}(\lambda)$  is derived by suitable high-pass filtering of the measured intensity  $I(\lambda)$ . The corresponding differential absorption cross sections  $\sigma'_j(\lambda)$  are determined by applying the same high-pass filter to  $\sigma_j(\lambda)$ , which in turn are measured in the laboratory (i.e. usually taken from the literature). The terms of the left hand side of Eq. (9) are measured, and then the atmospheric trace gas concentrations  $c_j$  are derived from  
 10 a least squares fit (details can be found in the above mentioned DOAS book). A separation of the different absorptions contributing to the sum in equation Eq. 9 is possible because the structures of the trace gases are unique, like a fingerprint.

While this formalism works well for long-path (active) DOAS applications, important modifications are required for its application for CE-DOAS. The problem is the dependence of the light path on the trace gas absorption. This can be clarified by considering  
 15 a situation with mirrors of infinitely good reflectance ( $R=1$ ) and vanishing extinction by species other than the trace gas to be measured. In this case the quality factor of the cavity and thus the effective light path length  $L_{\text{eff}}$  would only be determined by the trace gas concentration  $c$ , in fact we would have  $L_{\text{eff}} \propto 1/c$ . Since the optical density  
 20 due to the trace gas is proportional to  $c \times L_{\text{eff}}$  we would have:  $D \propto c \times L_{\text{eff}} \propto 1/c \times c = 1$ , i.e.  $D$  becomes independent of  $c$ . Under these conditions DOAS measurements are clearly impossible. In practice, these conditions are – fortunately – never met, however we have to conclude that too high mirror reflectivities can actually reduce the signal and that (sometimes considerable) corrections for the reduction of  $L_0$  due to trace gas

**High finesse optical resonators for DOAS measurements**

J. Meinen et al.

Title Page

Abstract

Introduction

Conclusions

References

Tables

Figures



Back

Close

Full Screen / Esc

Printer-friendly Version

Interactive Discussion



absorptions have to be made. The required corrections are described by Eq. (11), the justification of which will be detailed in the above mentioned theory paper. Moreover, the calculation of the optimum mirror reflectivity also has to consider the above effect of the trace gas absorption – dependent light path length. To our knowledge the corrections were not made in earlier studies (e.g. Fiedler et al., 2003, Ball et al., 2004, Langridge et al., 2006, Venables, et al., 2006, Ruth et al., 2007).

## 4 Results

This section presents the results of proof of principle measurements performed on gas phase absorbers in the laboratory and at the intercomparison campaign in the SAPHIR atmosphere simulation chamber. Laboratory measurements on NO<sub>2</sub>/NO<sub>3</sub> mixtures are shown first to demonstrate the sufficient spectral coverage of the instrument.

### 4.1 Laboratory measurements

NO<sub>3</sub> was synthesized in a continuous flow reactor in the reaction sequence NO+O<sub>3</sub>→NO<sub>2</sub>+O<sub>2</sub> and NO<sub>2</sub>+O<sub>3</sub>→NO<sub>3</sub>+O<sub>2</sub> (Atkinson et al., 2004). In order to achieve a complete NO to NO<sub>3</sub> reaction, we mixed a small fraction of NO (~15 ppmv) with a large quantity of O<sub>3</sub> (~350 ppmv) from an electrical discharge ozonizer in a constant flow of dry, filtered air at room temperature. The reaction occurred in a light sealed reaction chamber to avoid decomposition of the NO<sub>3</sub> due to photolysis. Reaction chamber and absorption chamber were made of glass and were connected by a 50 mm long Teflon tube. Tube and the absorption chamber were shielded from ambient light as well. The residence time in the reaction and absorption chamber were 15 s and 60 s, respectively. In spite of these precautions, NO<sub>2</sub> was always detectable in the absorption chamber. A typical CEAS spectrum is shown in Fig. 3. The transmitted intensity with and without an absorber inside the resonator is depicted and compared to the transmission characteristics of the mirrors. The 662 nm absorption band of NO<sub>3</sub> is lo-

## High finesse optical resonators for DOAS measurements

J. Meinen et al.

Title Page

Abstract

Introduction

Conclusions

References

Tables

Figures

⏪

⏩

◀

▶

Back

Close

Full Screen / Esc

Printer-friendly Version

Interactive Discussion



cated in the center of the LED emission spectrum and completely in the high reflecting region of the mirrors. Figure 4 shows the feasibility to detect  $\text{NO}_3$  in the presence of a large background of  $\text{O}_3$ . Concentrations of 0.31 ppbv  $\text{NO}_3$  in 590 ppmv  $\text{O}_3$  can be estimated roughly by using Eq. (3) with  $L_0=11.72$  km and nonlinear least-squares fit to the absorption coefficient:

$$a(\lambda) = n_{\text{O}_3} \times \sigma_{\text{O}_3}(\lambda) + n_{\text{NO}_3} \times \sigma_{\text{NO}_3}(\lambda) + T(\lambda) \quad (10)$$

In Eq. (10) the number densities  $n_{\text{O}_3}$  and  $n_{\text{NO}_3}$  [ $\text{cm}^{-3}$ ] are fit parameters.  $\sigma_{\text{O}_3}(\lambda)$  and  $\sigma_{\text{NO}_3}(\lambda)$  are taken from the literature for  $T=293$  K and  $T=294$  K respectively (UV-VIS Absorption Spectra of Gaseous Molecules and Radicals: <http://www.atmosphere.mpg.de/enid/2295/>, accessed: 2~November~2007.), and  $T(\lambda)$  is a polynomial representing instrumental effects. The residual is mainly caused by  $\text{NO}_2$  and water absorption and nonlinear effects of the light source and detection unit.

## 4.2 Intercomparison measurements in the SAPHIR chamber

In order to demonstrate its ability to detect  $\text{NO}_3$  under more realistic conditions, the instrument took part in an  $\text{N}_2\text{O}_5/\text{NO}_3$  intercomparison campaign at the SAPHIR atmosphere simulation chamber in Jülich. The goal of this campaign was to detect sub 100 ppt concentration of  $\text{NO}_3$  in the presence of water, aerosol and other trace gases.

The CEAS instrument was placed directly inside the chamber to avoid inlet losses. Under these conditions, an effective absorption path length of about 8500 m was determined by measuring the ring-down signal when the chamber was filled with synthetic air only. The path length varied slightly from day to day and therefore was determined prior to each experiment. The estimated uncertainty was <3%. During the experiment, spectra were acquired with a rate of  $0.2 \text{ min}^{-1}$  by the Mini-DOAS spectrometer described in Sect. 2. The exposure time typically was about 60 s but was varied automatically to reach constant illumination for all spectra. The data are handled and evaluated by using the software DOASIS (Kraus, 2006). For maximum data reliability, we defined two criteria when the data has to be discarded: First, when the background

### High finesse optical resonators for DOAS measurements

J. Meinen et al.

Title Page

Abstract

Introduction

Conclusions

References

Tables

Figures

◀

▶

◀

▶

Back

Close

Full Screen / Esc

Printer-friendly Version

Interactive Discussion



signal was dominating due to increased scattered light e.g. caused by an opened roof of the chamber. Second, when the fan inside the chamber was turned off, since than the purge flow and wall effects diluted the trace gas concentration between the mirrors in an unpredictable way.

Figure 5 shows raw data recorded from the spectrometer. To obtain low noise background spectra ( $I_0$ ) a total of 572 spectra were recorded, scaled and averaged overnight (Fig. 5a). During experiment, five subsequent spectra ( $I$ ) were averaged to maintain sufficient temporal resolution (Fig. 5b). Figure 6 demonstrates how the concentrations are determined by differential fitting to a broadband spectrum smoothed by a low pass filter. The fit shows a good match to the data in the region of high mirror reflectivity (635–680 nm). The concentration retrieved from this spectrum where  $c_{\text{NO}_3} = (631 \pm 5.48)$  pptv,  $c_{\text{H}_2\text{O}} = (955 \pm 255)$  ppmv and  $c_{\text{O}_3} = (7.51 \pm 0.82)$  ppmv. The uncertainty given here is the  $2\sigma$  statistical error associated with the spectral fit.  $\text{NO}_2$  was not detectable on this experiment day. The amount of  $\text{O}_3$  has to be interpreted with care. This absorber has a broad absorption structure in this wavelength range which can lead to misinterpretation in the DOAS approach.

Figure 7 shows time series for  $\text{NO}_3$  concentrations during one experiment day.  $\text{NO}_2$  and  $\text{O}_3$  were injected into the light sealed chamber to synthesize a certain amount of  $\text{NO}_3$ . Once the designated concentration was reached, the light shield of the chamber was opened to destroy the  $\text{NO}_3$  by photolysis. Such photolysis experiments were repeated several times at different concentrations, the corresponding breakdown is clearly visible in our data. Each point in Fig. 7 represents the mean of five spectra recorded. This gives a temporal resolution of 6 min, not sufficient to resolve the dynamics of the single photolysis events in time. The data point marked by an arrow was obtained by analyzing the data shown in Figs. 5 and 6 (same in Fig. 8).

The evaluation of the data yields a  $1\text{-}\sigma$  accuracy of the CE–DOAS  $\text{NO}_3$  measurement from 6.3 to 13 pptv at days without high aerosol and high water values (see dotted line in Fig. 7). True  $\text{NO}_3$  concentrations  $\bar{c}$  were calculated from the column densities  $D'$  considering the light path reduction caused by the column density itself and the

---

## High finesse optical resonators for DOAS measurements

J. Meinen et al.

---

[Title Page](#)[Abstract](#)[Introduction](#)[Conclusions](#)[References](#)[Tables](#)[Figures](#)[◀](#)[▶](#)[◀](#)[▶](#)[Back](#)[Close](#)[Full Screen / Esc](#)[Printer-friendly Version](#)[Interactive Discussion](#)

uncorrected concentration  $\bar{c}_0$  derived from the DOAS fit (see above mentioned theory paper).

$$\bar{c} = \bar{c}_0 \frac{1}{1 - D'} \quad (11)$$

This correction is crucial in all cavity enhanced approaches and in our measurement can amount up to 15% for  $\text{NO}_3$  concentrations around 300 ppvt. A well defined correlation is not achievable without this correction, especially at high extinctions. The good performance of our simple instrument is demonstrated by comparing it to a reference instrument employing a traditional long path DOAS using a white cell (Dorn et al., 1995). In Fig. 8 the correlation plot between the two instruments show a very high correlation coefficient  $R=0.98$ , a constant of proportionality of  $1.03 \pm 0.01$  and no offset between the two instruments.

Common to all cavity enhanced approaches is the varying light path length  $L_0$  inside the cavity as discussed in Sect. 3.2. This reduction of the light path is not only caused by the target species itself, which can be corrected by Eq. (11), but also by extinction caused by varying concentrations of background aerosol. Depending on the measurement principle, there are different approaches to cope with this problem: (1) In single wavelength CRD or CEA one has to remove the aerosol by filtering the analyte and additionally remove the species to be measured by titration, thermal decomposition or photolysis to measure the absolute zero signal. Especially filtering the analyte has the severe drawback that unstable species, e.g.  $\text{NO}_3$ , may be lost. In multi wavelength or broadband approaches, there are three possibilities to solve the problem: (2) Filtering of the analyte to achieve a direct measure of the absorption without any scattering. (3) Titration, thermal decomposition or photolysis to remove the trace species for a background which can be subtracted from the signal. (4) Relation of the concentration of the trace species to a known concentration of other absorber e.g.  $\text{O}_2$ ,  $\text{O}_4$  or  $\text{H}_2\text{O}$ . In this case one can easily determine the aerosol extinction additionally.

In the measurements presented here, we operated principally in mode (2). In the laboratory test case, we synthesized our analyte from gas bottles and sampled it di-

## High finesse optical resonators for DOAS measurements

J. Meinen et al.

Title Page

Abstract

Introduction

Conclusions

References

Tables

Figures

◀

▶

◀

▶

Back

Close

Full Screen / Esc

Printer-friendly Version

Interactive Discussion



rectly into the cavity. Thus no aerosol was able to emerge. During the intercomparison campaign at the SAPHIR chamber the cavity was mounted directly inside the chamber and thus it was accessible to all species which were filled into the chamber for the experiments. In this report, we confined ourselves to the analysis of the data with extreme low or at least low and constant aerosol concentrations. On experiment days with moderate and high aerosol concentrations special corrections have to be concerned in the analysis. This will be described in detail in the theory paper mentioned above.

The total measurement uncertainty is estimated to be better than 15%. This value is made up from the following contributions: The geometrical light path  $L_0$ , which is determined by fitting a simple exponential function to the ring-down signal. By doing so,  $L_0$  has an uncertainty of smaller than 3%. Furthermore the effective absorption path length  $d_0$  is determined by the pure flow of each mirror. The fraction of  $d$  affected by the purge flow is 6 cm for each mirror with an uncertainty of about 20% or 1.2 cm at each end. This gives an uncertainty of 2.4 cm of the effective absorption path length between the two mirrors  $d_0$  which contributes about 5% to the total uncertainty. The fitting uncertainty in the DOAS evaluation is typically about 5%. Additionally, the uncertainty of the absorption cross section of the species has to be included in the absolute accuracy of the measurement. For the data set used herein, this is about 10% for  $\text{NO}_3$  (Yokelson et al., 1994). The correction for the reduced light path (cf. Eq. 11) contributes up to 3% additional uncertainty for high concentrations of  $\text{NO}_3$  (>300 pptv). At low concentrations (<50 pptv) this contribution is negligible in the context of these measurements. The uncertainties sum up to a total measurement uncertainty of about 13%. The detection limit of the instrument is given by twice the fit error of the DOASIS software. For experiments with low water vapor and aerosol concentrations a detection limit of about 6–13 pptv is achieved.

## High finesse optical resonators for DOAS measurements

J. Meinen et al.

Title Page

Abstract

Introduction

Conclusions

References

Tables

Figures

⏪

⏩

◀

▶

Back

Close

Full Screen / Esc

Printer-friendly Version

Interactive Discussion



## 5 Conclusions

In Cavity Enhanced Differential Optical Absorption Spectroscopy (CE-DOAS) the incoherent radiation of a LED with a relatively broad emission spectrum transmitted by an optical stable cavity is dispersed with a monochromator and detected by a CCD detector. In doing so, this method combines the advantages of sensitivity and specificity of standard non invasive in-situ Differential Optical Absorption Spectroscopy (DOAS) with the enhancement provided by the long light path of an optical resonator. All this is obtained in a very simple and compact setup. The CE-DOAS method is characterized by its insensitivity to both, intensity fluctuations of the light source and the varying background of scattering aerosol. The method employed here is distinguished from other cavity enhanced approaches by accounting for the reduction of the light path by the trace gas absorption. This is essential since cavity losses due to absorption by trace gases reduce the quality of the cavity. Reduction of the light path by aerosol extinction was neglected here since these concentration were extreme low or at least low and constant.

The LED light source covers a spectral range of  $\Delta\lambda\approx 23$  nm centered at 665 nm, and therefore is applicable for the detection of  $\text{NO}_3$  with a significant higher spatial resolution than in standard long-path DOAS systems. This can be done without the need of thermal decomposition or titration of the analyte as it is necessary in single wavelength approaches. With total exposure times of 60 s (total acquisition time of 300 s), the concentration of  $\text{NO}_3$  was measured at part per trillion dilution with a statistical uncertainty of  $\pm 6.3$  pptv and an rms noise of  $10^{-9} \text{ cm}^{-1}$  in the residual extinction spectrum.

One of the key limitations of obtaining high temporal resolution at sufficient signal to noise ratios is the amount of light coupled stably in the cavity. Caused by the conservation of radiance only a very small radiating area of the light source can be imaged into the stable region of the resonator. For this reason it is essential to choose a light source with high surface radiance. Some LEDs have promising performance, but they are outperformed by so called Superluminescent Light Emitting Diodes (SLD). These

### High finesse optical resonators for DOAS measurements

J. Meinen et al.

Title Page

Abstract

Introduction

Conclusions

References

Tables

Figures

◀

▶

◀

▶

Back

Close

Full Screen / Esc

Printer-friendly Version

Interactive Discussion



modified laser diodes have a broad ( $\Delta\lambda\approx 10$  nm) and nearly incoherent emission with a much higher surface luminance than LEDs have. SLDs share all advantages of conventional LEDs except their low cost. Prices of SLDs are comparable to high quality diode lasers. We started test measurements with 660 nm SLD and obtained first promising results. Upgrading our CE-DOAS device with a SLD light source will be the scope of a future publication.

*Acknowledgements.* The authors greatly appreciate the support by ACCENT for the intercomparison campaign at the atmosphere simulation chamber SAPHIR. Moreover the SAPHIR team is gratefully thanked for support during the campaign and for the supply of the data for Fig. 8. The authors thank Denis Pöhler and Holger Sihler for suggestions and advice in terms of the differential fitting utilizing DOASIS.

## References

- Atkinson, R., Baulch, D. L., Cox, R. A., Crowley, J. N., Hampson, R. F., Hynes, R. G., Jenkin, M. E., Rossi, M. J., and Troe, J.: Evaluated kinetic and photochemical data for atmospheric chemistry: Volume I – gas phase reactions of Ox, Hox, Nox and Sox species, 4, 1461–1738, 2004.
- Ball, S. M., Povey, I. M., Norton, E. G., and Jones R. L.: Broadband cavity ringdown spectroscopy of the NO<sub>3</sub> radical, Chem. Phys. Lett., 342, 113–120, 2001.
- Ball, S. M. and Jones, R. L.: Broad-Band Cavity Ring-Down Spectroscopy, Chem. Rev., 103, 5239–5262, 2003.
- Ball, S. M., Langridge, J. M., and Jones, R. L.: Broadband cavity enhanced absorption spectroscopy using light emitting diodes, Chem. Phys. Lett., 398, 68–74, 2004.
- Brown, S. S.: Absorption Spectroscopy in High-Finesse Cavities for Atmospheric Studies, Chem. Rev., 103, 5219–5238, 2003.
- Dorn, H.-P., Brandenburger, U., Brauers, T., and Hausmann, M.: A new in-situ laser long-path absorption instrument for the measurement tropospheric OH radicals., J. Atmos. Sci. 52, 3373–3380, 1995.
- Engeln, R., Berden, G., Peeters, R., and Meijer, G.: Cavity enhanced absorption and cavity enhanced magnetic rotation spectroscopy, Rev. Sci. Instrum., 69, 3763–3769, 1998.

## High finesse optical resonators for DOAS measurements

J. Meinen et al.

Title Page

Abstract

Introduction

Conclusions

References

Tables

Figures

◀

▶

◀

▶

Back

Close

Full Screen / Esc

Printer-friendly Version

Interactive Discussion



- Fiedler, S. E., Hese, A. and Ruth, A. A.: Incoherent broad-band cavity-enhanced absorption spectroscopy, Chem. Phys. Lett., 371, 284–294, 2003.
- Fiedler, S. E. and Hese, A.: Influence of the cavity parameters on the output intensity in incoherent broadband cavity-enhanced absorption spectroscopy, Rev. Sci. Instr., 78, 0731041–0731047, 2007.
- 5 Hamers, E., Schram, D. and Engeln, R.: Fourier transform phase shift cavity ring down spectroscopy, Chem. Phys. Lett., 265, 237–243, 2002.
- Herriot, D. R. and Schulte, H. J.: Folded Optical Delay Lines, Appl. Optics, 4, 883–889, 1965.
- Hönninger, G., Friedeburg, C. V., and Platt, U.: Multi axis differential optical absorption spectroscopy (MAX-DOAS), Atmos. Chem. Phys., 4, 231–254, 2004,  
<http://www.atmos-chem-phys.net/4/231/2004/>.
- 10 Kern, C., Trick, S., Rippel, B., and Platt, U.: Applicability of light-emitting diodes as light sources for active differential optical absorption spectroscopy measurements, Appl. Optics, 45, 2077–2088, 2006.
- 15 Kraus, S. G.: DOASIS, A Framework Design for DOAS., Doctoral Thesis, University of Heidelberg, Germany, see also: <http://www.iup.uni-heidelberg.de/bugtracker/projects/doasis/>, 2006.
- Langridge, J. M., Stephen, M. B., and Jones, R. L.: A compact broadband cavity enhanced absorption spectrometer for detection of atmospheric NO<sub>2</sub> using light emitting diodes, Analyst, 20 131, 916–922, 2006.
- O’Keefe, A., Scherer, J. J., and Paul, J. B.: cw Integrated cavity output spectroscopy, Chem. Phys. Lett., 307, 343–349, 1999.
- Paul, J. B., Lapson, L. and Anderson, J. G.: Ultrasensitive absorption spectroscopy with a high-finesse optical cavity and off-axis alignment, Appl. Optics, 40, 4904–4910, 2001.
- 25 Platt, U. and Perner, D.: Direct measurements of atmospheric CH<sub>2</sub>O, HNO<sub>2</sub>, O<sub>3</sub>, NO<sub>2</sub>, SO<sub>2</sub> by differential optical absorption in the near UV, J. Geophys. Res., 85, 7453–7458, 1980.
- Ruth, A. A., Orphal, J., and Fiedler, S. E.: Fourier-transform cavity-enhanced absorption spectroscopy using an incoherent broadband light source, Appl. Optics, 46, 3611–3616, 2007.
- Simpson, W. R.: Continuous wave cavity ring-down spectroscopy applied to in situ detection of dinitrogen pentoxide (N<sub>2</sub>O<sub>5</sub>), Rev. Sci. Instr., 74, 1–11, 2003.
- 30 Sneep, M. and Ubachs, W.: Direct measurement of the Rayleigh scattering cross section in various gases, J. Quant. Spectrosc. Ra., 92, 293–310, 2005.
- Venables, D. S., Gherman, T., Orphal, J., Wenger, J. C., and Ruth, A. A.: High Sensitive in

---

## High finesse optical resonators for DOAS measurements

J. Meinen et al.

---

Title Page

Abstract

Introduction

Conclusions

References

Tables

Figures

◀

▶

◀

▶

Back

Close

Full Screen / Esc

Printer-friendly Version

Interactive Discussion



Situ Monitoring of NO<sub>3</sub> in an Atmospheric Simulation Chamber Using Incoherent Broadband Cavity-Enhanced Absorption Spectroscopy, *Environ. Sci. Technol.*, 40, 6758–6763, 2006.

White, J. U.: Long optical paths of large aperture, *J. Opt. Soc. Am.*, 32, 285–288, 1942.

5 Yokelson, R. J., Burkholder, J. B., Fox, R. W., Talukdar, R. K., and Ravishankara, A. R.: Temperature Dependence of the NO<sub>3</sub> Absorption Spectrum, *J. Phys. Chem.*, 98, 13144–13150, 1994.

ACPD

8, 10665–10695, 2008

---

## High finesse optical resonators for DOAS measurements

J. Meinen et al.

---

Title Page

Abstract

Introduction

Conclusions

References

Tables

Figures

◀

▶

◀

▶

Back

Close

Full Screen / Esc

Printer-friendly Version

Interactive Discussion



## High finesse optical resonators for DOAS measurements

J. Meinen et al.

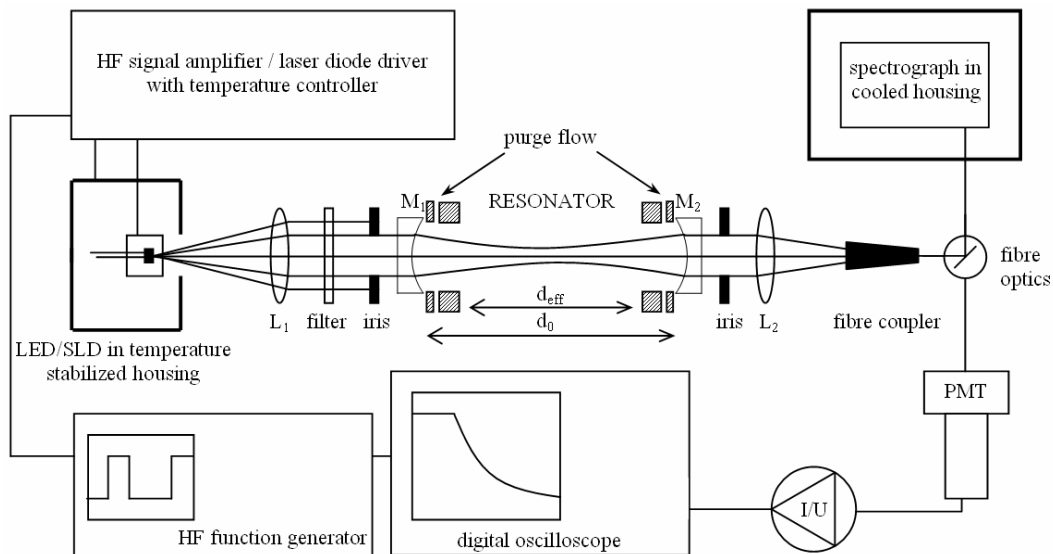


**Fig. 1.** Schematic diagram of the LED/SLD-based experimental setup used for CE-DOAS.  $L_1$  and  $L_2$ : lenses;  $M_1$  and  $M_2$ : high reflectivity dielectric mirrors with  $R \approx 0.99998$  at 655 nm; Filter: Schott RG610 3 mm.

Title Page

Abstract

Introduction

Conclusions

References

Tables

Figures

◀

▶

◀

▶

Back

Close

Full Screen / Esc

Printer-friendly Version

Interactive Discussion



**High finesse optical resonators for DOAS measurements**

J. Meinen et al.

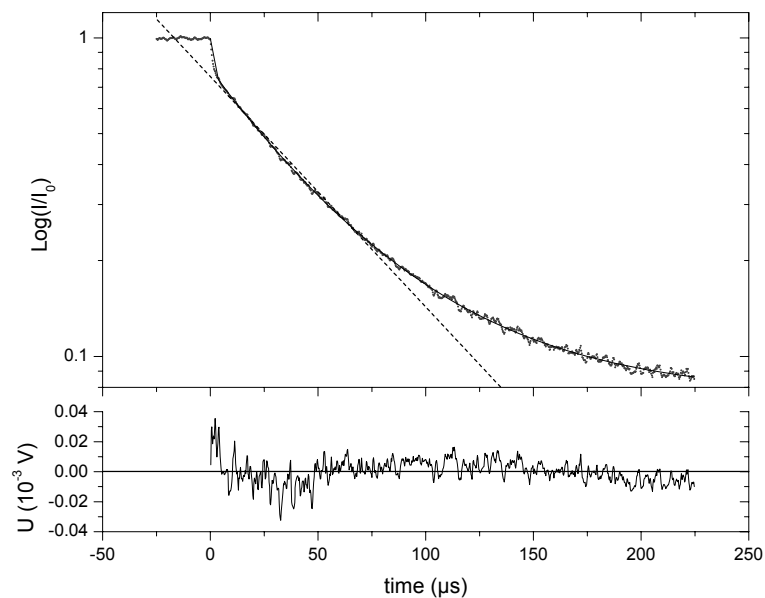


**Fig. 2.** Ring-down signal averaged from 1000 cycles. Small dots: measurement data. Solid line: multi-exponential fit (0–225 μs). Dashed line: single-exponential fit (5–75 μs). Lower panel: fit residual of multi-exponential fit. Note non-linear decay of  $\text{Log}(I/I_0)$ .

[Title Page](#)[Abstract](#)[Introduction](#)[Conclusions](#)[References](#)[Tables](#)[Figures](#)[◀](#)[▶](#)[◀](#)[▶](#)[Back](#)[Close](#)[Full Screen / Esc](#)[Printer-friendly Version](#)[Interactive Discussion](#)

## High finesse optical resonators for DOAS measurements

J. Meinen et al.

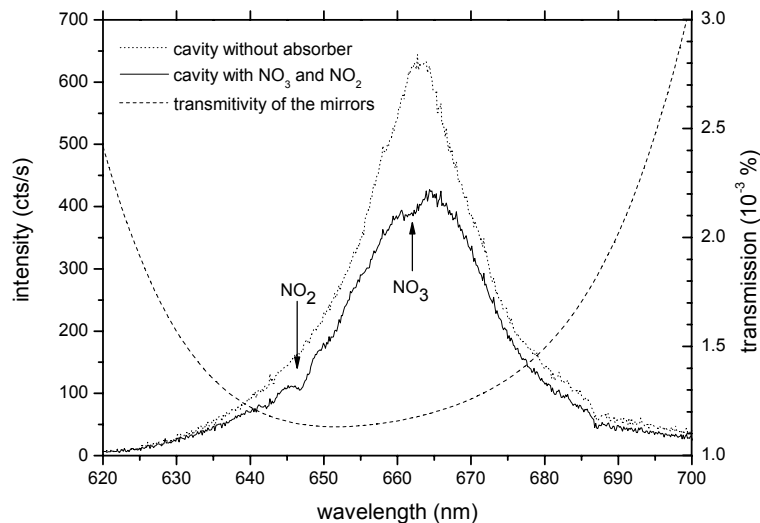


**Fig. 3.** Transmitted intensity of the resonator: Integration time  $10 \times 5$  s. The dotted line shows the transmitted intensity of the empty cavity, which is the LED emission spectrum folded by the mirror transmission. The solid line was recorded with approx. 0.3 ppbv  $\text{NO}_3$  and 810 ppbv  $\text{NO}_2$ . Transmissivity of the high reflective mirrors.

Title Page

Abstract

Introduction

Conclusions

References

Tables

Figures

◀

▶

◀

▶

Back

Close

Full Screen / Esc

Printer-friendly Version

Interactive Discussion



**High finesse optical resonators for DOAS measurements**

J. Meinen et al.

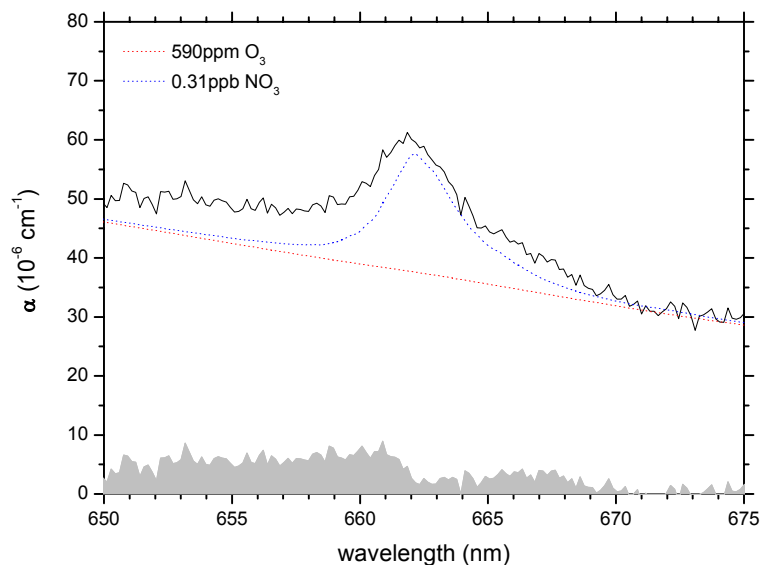


**Fig. 4.** Detection of  $\text{NO}_3$  in a large background of  $\text{O}_3$  in air. The solid line shows the absorption coefficient of the samples calculated by conventional CEAS means from the data shown in Fig. 3. The offset is due to absorption of 590 ppm Ozone in the cavity (dotted, red). The  $\text{NO}_3$  peak is due to a concentration of 0.31 ppb (dotted, blue). Residual (mainly from  $\text{NO}_2$ , grey). This rough estimation of concentration based on Eq. 3 and Eq. 10 coincides with the DOAS analysis results.

Title Page

Abstract

Introduction

Conclusions

References

Tables

Figures

◀

▶

◀

▶

Back

Close

Full Screen / Esc

Printer-friendly Version

Interactive Discussion



## High finesse optical resonators for DOAS measurements

J. Meinen et al.

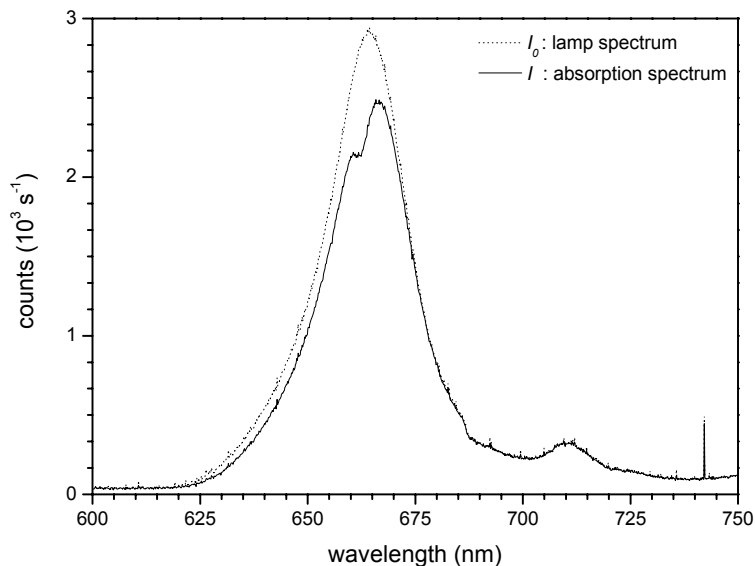


**Fig. 5.** Recorded CE-DOAS spectra during the  $\text{NO}_3/\text{N}_2\text{O}_5$  intercomparison campaign (transmitted intensity of the resonator). **(a)**  $I_0$  (lamp) spectra were recorded overnight by averaging 572 scaled spectra (dotted line). **(b)** During experiments five spectra were averaged (solid line). This absorption spectrum ( $I$ ) shows the attenuation corresponding to 631 pptv  $\text{NO}_3$ .

[Title Page](#)[Abstract](#)[Introduction](#)[Conclusions](#)[References](#)[Tables](#)[Figures](#)[◀](#)[▶](#)[◀](#)[▶](#)[Back](#)[Close](#)[Full Screen / Esc](#)[Printer-friendly Version](#)[Interactive Discussion](#)

## High finesse optical resonators for DOAS measurements

J. Meinen et al.

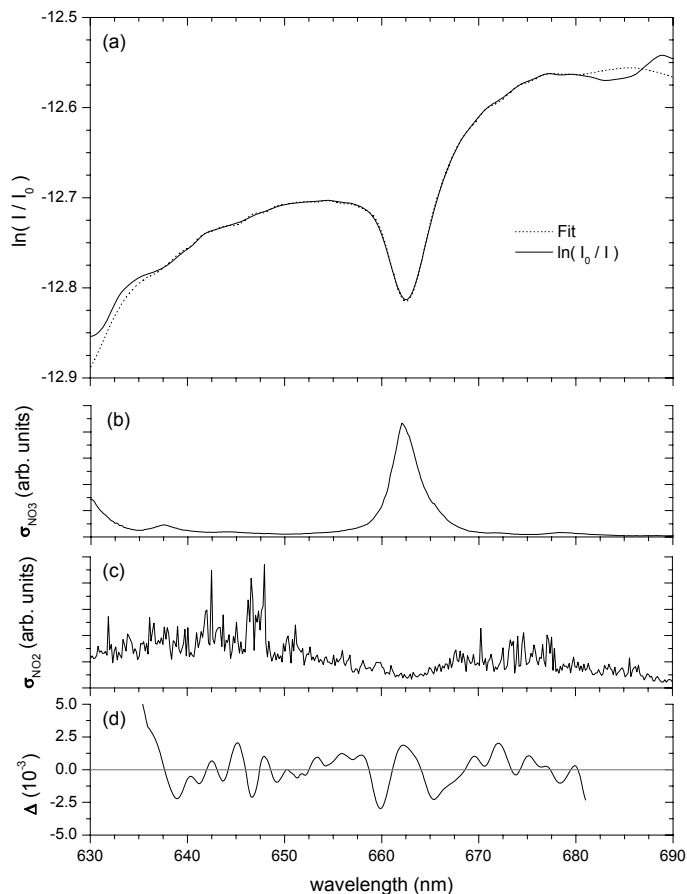


**Fig. 6.** CE-DOAS spectra of 631 pptv  $\text{NO}_3$  with traces of  $\text{NO}_2$ ,  $\text{O}_3$  and  $\text{H}_2\text{O}$ . Panel (a) shows the measured spectrum smoothen with a low pass filter (solid line) and overlaid by the fit result (dotted line). Panel (d) shows the residual spectrum in the data region relevant for the fit. Panel (b) and (c) show the absorption cross sections from  $\text{NO}_3$  and  $\text{NO}_2$ , respectively.

[Title Page](#)[Abstract](#)[Introduction](#)[Conclusions](#)[References](#)[Tables](#)[Figures](#)[◀](#)[▶](#)[◀](#)[▶](#)[Back](#)[Close](#)[Full Screen / Esc](#)[Printer-friendly Version](#)[Interactive Discussion](#)

**High finesse optical resonators for DOAS measurements**

J. Meinen et al.

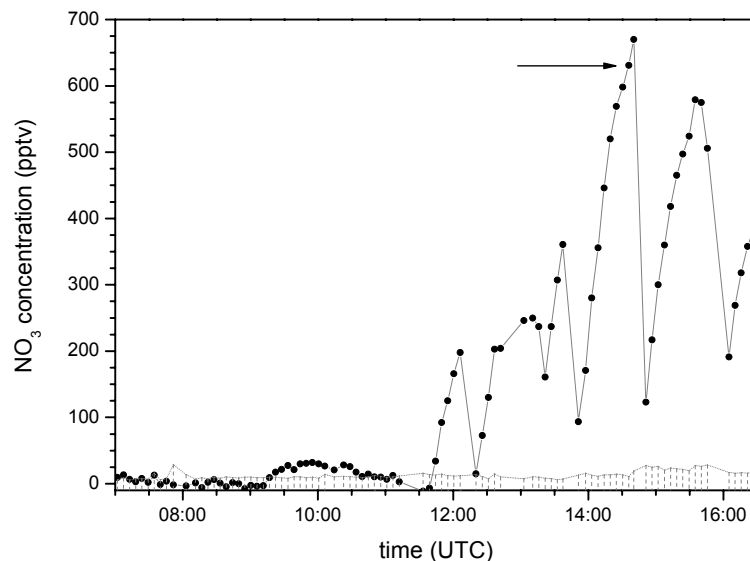


**Fig. 7.** Time series for NO<sub>3</sub> concentration of one experiment day. Each point represents a concentration accessed by DOAS analysis. The dotted line represents the 1 $\sigma$  uncertainty of the individual fit result. The data point marked by an arrow was obtained by analyzing the data shown in Figs. 5 and 6.

[Title Page](#)[Abstract](#)[Introduction](#)[Conclusions](#)[References](#)[Tables](#)[Figures](#)[◀](#)[▶](#)[◀](#)[▶](#)[Back](#)[Close](#)[Full Screen / Esc](#)[Printer-friendly Version](#)[Interactive Discussion](#)

**High finesse optical resonators for DOAS measurements**

J. Meinen et al.

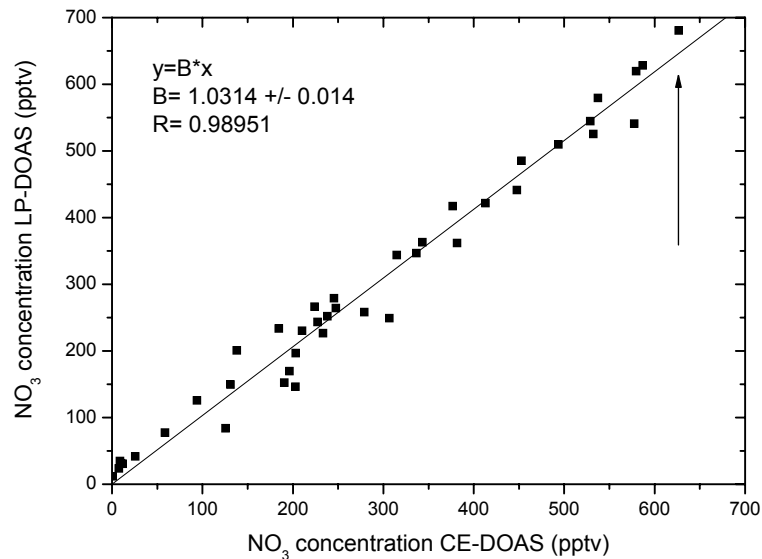


**Fig. 8.** Correlation plot for NO<sub>3</sub> concentrations accessed by the CE-DOAS device and the reference long path DOAS device of the SAPHIR atmosphere simulation chamber. The data point marked by an arrow was obtained by analyzing the data shown in Figs. 5 and 6.

[Title Page](#)[Abstract](#)[Introduction](#)[Conclusions](#)[References](#)[Tables](#)[Figures](#)[◀](#)[▶](#)[◀](#)[▶](#)[Back](#)[Close](#)[Full Screen / Esc](#)[Printer-friendly Version](#)[Interactive Discussion](#)